Available online at www.sciencedirect.com
ScienceDirect
Journal of Power Sources 164 (2007) 713–720
JOURNAL OF POWER SOURCES
www.elsevier.com/locate/jpowsour

Temperature control of MCFC based on an affine nonlinear thermal model

Fan Yang *, Xin-Jian Zhu, Guang-Yi Cao

Fuel Cell Research Institute, Shanghai JiaoTong University, Shanghai 200030, China

Received 27 September 2006; received in revised form 28 October 2006; accepted 17 November 2006
Available online 4 January 2007

Abstract

The molten carbonate fuel cell (MCFC) is a promising device for stationary power and heat supply. In this work, the temperature control in MCFC stack is studied. The operating temperature of the stack is an important controlled variable, which impacts the performance of the MCFC due to thermal cycling. In order to improve the generating performance of the MCFC, prolong its life and guarantee safety, credibility and low degradation of the fuel cell, the temperature of MCFC must be controlled efficiently. Based on analyzing the temperature dynamic model of MCFC, a model-based variable structure control (VSC) controller is designed for MCFC in this paper. The optimal parameters of VSC are selected by genetic algorithm (GA). Numerical results demonstrate the effectiveness and advantages of this approach.

Keywords: Molten carbonate fuel cell; Variable structure control; Genetic algorithm

1. Introduction

The molten carbonate fuel cell is a promising device for stationary power and heat supply and has been continuously developing by many countries including USA, Japan, and Korea. It was demonstrated by several manufacturers that in the sub-MW region MCFC power plants can reach electrical efficiencies of 47%. By making use of the heat generated by the system, total efficiencies of more than 80% can be achieved [1].

Performance and availability of MCFC stack are greatly dependent on its operating temperature. Due to its high operating temperature of about 873 K, this concept has certain advantages over low-temperature fuel cell systems. The temperature is high enough to allow for internal reforming, which means to produce hydrogen from different types of fuel gases within the cell stack itself. Also due to the high temperature, no expensive catalysts are required; nickel and nickel oxide are sufficiently active as electrode catalysts. However, when the operating temperature is higher than 973 K, material corrosion accelerates greatly, and electrolyte loss increases, which increases the risk of short-circuit and shortens the stack lifespan [2]. Consequently, it is crucial for improving the performance and life of the fuel cell that the operating temperature be controlled in an appropriate range.

For getting a better thermal management of MCFC stack, it is necessary to develop the thermal model, and find the suitable control method based on this model. Over the last decade, many researchers all over the world have made great progress on MCFC modeling to improve its performance and cost competitiveness with energy conversion devices currently available. Various mathematical models have been established in the research on the internal mechanisms, ranging from a one dimensional non-isothermal model to a three dimensional non-isothermal and non-isobaric models [3–6], but the most existing models of MCFC are not ready to be applied in synthesis. In Ref. [7], a nonlinear mathematical model of an internal reforming MCFC stack is developed for control system. In Ref. [8] a control-oriented quantitative relation model of MCFC is developed between the temperatures of the stack and flow rates of the input gases. However, temperature control is only mentioned and the model-based control strategy is not discussed.

As above mentioned, it is necessary to develop a simple model, and find suitable control method for dynamic thermal transfer. In this paper, we analyze the dynamic thermal transfer model of MCFC stack based on the modeling of Shen [8]. This model is nonlinear with disturbances and uncertainty as

* Corresponding author. Tel.: +86 21 28164995; fax: +86 21 62932154.
E-mail address: yangfantracy@hotmail.com (F. Yang).

0378-7753/$ – see front matter © 2006 Elsevier B.V. All rights reserved.
doi:10.1016/j.jpowsour.2006.11.027

Nomenclature

A	area of heat exchange (m^2)
c	mass heat capacity ($J\,kg^{-1}\,K^{-1}$)
C	heat capacity ($J\,K^{-1}$)
F	Faraday constant ($26.8\,A\,h\,mol^{-1}$)
j	local current density ($A\,m^{-2}$)
k	local heat-transfer rate coefficients ($J\,S^{-1}\,m^{-2}\,K^{-1}$)
q	energy rate available from the input fuel and oxidant gas ($J\,S^{-1}\,K^{-1}$)
q_{H_2O}	heat generation of 1 M H_2O ($J\,mol^{-1}$)
Q	heat energy
r	heat radiation coefficient
S	cross-section area of the flow channel of fuel and oxidant gas (m^2)
T	temperature (K)
u	flow-rate of gas ($m\,s^{-1}$)
V	operating voltage of the cell (V)
w_c	width of cells (m)

Greek letter

ρ	density ($kg\,m^{-3}$)

Subscripts

e	electrode–electrolyte plate
ef	between fuel gas and electrode–electrolyte plate
eo	between oxidant gas and electrode–electrolyte plate
es	between electrode–electrolyte plate and separator
f	fuel gas
in_f	original quantity of the fuel gas at the inlet
o	oxidant gas
in_o	original quantity of the oxidant gas at the inlet
s	separator
sf	between fuel gas and separator
so	between oxidant gas and separator

shown later in this paper. However, the performance of generalized controller largely depends on the availability of an accurate model. As a consequence, the application of conventional control strategies leads to unacceptable closed loop performances. The controller must be robust to uncertainty in a non-conservative manner and must meet closed-loop objectives such as tracking, regulation and disturbance attenuation.

Variable structure control systems (VSC) [12,13] constitute an important class of control systems. The main advantage of VSC is the possibility of obtaining a trajectory describing a new type of motion called 'sliding regime' or 'sliding mode', which is not inherent in any of the original structures. Sliding mode is defined as the motion of the system state along the switching surface that is not a trajectory of any of the structures. In the sliding mode, the system dynamics are independent of system parameters and external disturbances. As a consequence, based on VSC systems some works have been reported for the model-following control systems [14–16]. In this paper, the variable structure control (VSC) algorithm with a rapid-smooth reaching law and rapid-convergent sliding mode [17] is used to control the operating temperature within a specified range and reducing temperature fluctuation. The input/output linearization method is introduced into the affine nonlinear system and then a decentralized variable structure control system is constructed. Genetic algorithm (GA) is used to optimize the parameters of the decentralized VSC, including the parameters of the sliding mode and ones of the reaching law. Satisfactory simulation results are obtained.

The organization of this paper is as follows. The affine nonlinear model with multi-input and multi-output is given in the next section. Section 3 gives the design of the variable structure control (VSC) in detail. In Section 4, numerical simulations are presented to test the validity of the proposed controller. Finally, we present our concluding remarks.

2. Dynamic thermal transfer model of MCFC stack

2.1. Description and analysis of MCFC

A single cell consists of anode, cathode, electrolyte plate, separator plates, corrugated plates and current collectors. Fuel and oxidant gas flow in the anode and cathode channels along the corrugated plates. O_2 and CO_2 in oxidant gas react with electron at the cathode, and produce ${CO_3}^{2-}$. ${CO_3}^{2-}$ moves within the electrolyte plate perpendicularly from cathode side to anode side driven by the force of concentration difference. At the anode, H_2 in fuel gas reacts with ${CO_3}^{2-}$, which produces CO_2, H_2O and electrons by electro-chemical reaction. Released electrons are collected by the current collector and then pass the corrugated plate and separator perpendicularly. The top and the bottom separators are connected to external load equipment [9]:

$$\text{anode}: \quad H_2 + {CO_3}^{2-} \rightarrow CO_2 + H_2O + 2e^-,$$

$$\text{cathode}: \quad 4e^- + 2CO_2 + O_2 \rightarrow 2{CO_3}^{2-},$$

$$\text{overall reaction}: \quad 2H_2 + O_2 \rightarrow 2H_2O$$

The temperature of stack is mainly affected by the flow rate of inlet gas [11]. Slow flowing of gases leads to an adequate reaction, less heat lost and heat produced. On the other hand, fast flowing of gases results in an inadequate reaction, much more heat flown away with the remnant gases, and much reaction heat produced. Therefore, the steady temperature of the stack varies with the flow-rate of feeding gas of anode and cathode in a complex manner. In general, in order to cool the stack and make the fuel to be utilized to the maximum limited fuel utilization at most, it is assumed that the oxidant (i.e. compressed air to cathode) is abundant.

2.2. Dynamic thermal transfer of MCFC stack

In this section, the proposed dynamic thermal transfer model of MCFC is based on the following assumptions:

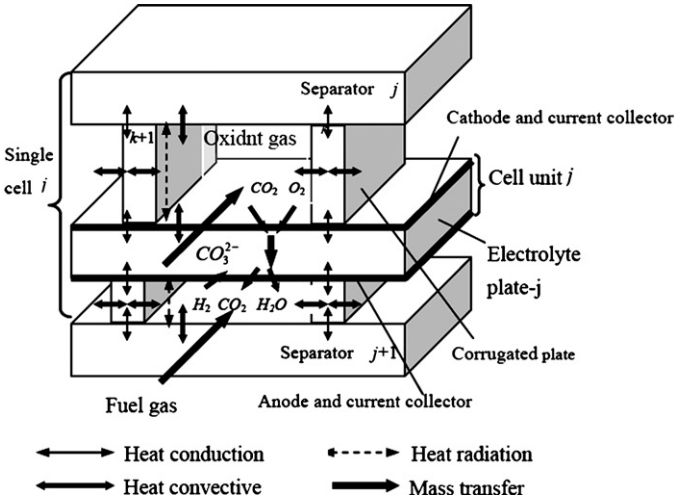

Fig. 1. Process of mass transport and heat generation and transfer in a MCFC cell.

- The composition change of fuel and oxidant gas because of the shift reactions in the cells can be ignored.
- The stack boundary is isothermal.
- External reforming, co-flow type stack, and the gases flow in smooth-walled channels of constant cross-section.
- The gases flow fast in short channels, and so the heat conduction inside the gases along the flow direction, horizontal heat conduction of electrode–electrolyte plates and separators can be ignored.

There are mainly the following heat transfer processes in an MCFC stack as shown in Fig. 1:

(a) the input heat energy of fuel gas;
(b) heat convection between fuel gas and electrode–electrolyte plate;
(c) heat convection between fuel gas and separator plate;
(d) the input heat energy of oxidant gas;
(e) heat convection between oxidant gas and electrode–electrolyte plate;
(f) heat convection between oxidant gas and separator plate;
(g) heat generation of water in the reaction;
(h) ohmic heat because of electric current;
(i) heat radiation between electrode–electrolyte plate and separator.

Mass and energy balance analysis [10] is performed on the fuel gas, oxidant gas, electrolyte plate and separator and the following relations can be obtained [8].

2.2.1. Fuel gas

The temperature of fuel gas is affected by the heat transfer processes (a), (b) and (c). A heat balance is written:

$$C_{\mathrm{f}}\frac{\mathrm{d}T_{\mathrm{f}}}{\mathrm{d}t} = Q_{\mathrm{in\_f}} + Q_{\mathrm{ef}} + Q_{\mathrm{sf}} \tag{1}$$

where

$$Q_{\mathrm{in\_f}} = q_{\mathrm{f}}(T_{\mathrm{in\_f}} - T_{\mathrm{f}}), \qquad Q_{\mathrm{ef}} = k_{\mathrm{ef}}A(T_{\mathrm{e}} - T_{\mathrm{f}}),$$
$$Q_{\mathrm{sf}} = k_{\mathrm{sf}}A(T_{\mathrm{s}} - T_{\mathrm{f}}), \quad C_{\mathrm{f}} = c_{\mathrm{f}}\rho_{\mathrm{f}}s_{\mathrm{f}}w, \quad q_{\mathrm{f}} = c_{\mathrm{in\_f}}\rho_{\mathrm{in\_f}}s_{\mathrm{f}}u_{\mathrm{f}}$$

2.2.2. Oxidant gas

The temperature of oxidant gas is affected by the heat transfer processes (d), (e) and (f). A heat balance is written:

$$C_{\mathrm{o}}\frac{\mathrm{d}T_{\mathrm{o}}}{\mathrm{d}t} = Q_{\mathrm{in\_o}} + Q_{\mathrm{eo}} + Q_{\mathrm{so}} \tag{2}$$

where

$$Q_{\mathrm{in\_o}} = q_{\mathrm{o}}(T_{\mathrm{in\_o}} - T_{\mathrm{o}}), \qquad Q_{\mathrm{eo}} = k_{\mathrm{eo}}A(T_{\mathrm{e}} - T_{\mathrm{o}}),$$
$$Q_{\mathrm{so}} = k_{\mathrm{so}}A(T_{\mathrm{s}} - T_{\mathrm{o}}), \quad C_{\mathrm{o}} = c_{\mathrm{o}}\rho_{\mathrm{o}}s_{\mathrm{o}}w, \quad q_{\mathrm{o}} = c_{\mathrm{in\_o}}\rho_{\mathrm{in\_o}}s_{\mathrm{o}}u_0$$

2.2.3. Electrode–electrolyte plate

The temperature of electrode–electrolyte plate is affected by the heat transfer processes (b), (e), (g), (h) and (i). A heat balance is written:

$$C_{\mathrm{e}}\frac{\mathrm{d}T_{\mathrm{e}}}{\mathrm{d}t} = Q_{\mathrm{fe}} + Q_{\mathrm{oe}} + Q_{\mathrm{H_2O}} + Q_{\mathrm{ohmic}} + Q_{\mathrm{se}} \tag{3}$$

where

$$Q_{\mathrm{fe}} = k_{\mathrm{ef}}A(T_{\mathrm{f}} - T_{\mathrm{e}}), \qquad Q_{\mathrm{oe}} = k_{\mathrm{eo}}A(T_{\mathrm{o}} - T_{\mathrm{e}}),$$
$$Q_{\mathrm{H_2O}} = \frac{jA}{2F}q_{\mathrm{H_2O}}, \qquad Q_{\mathrm{ohmic}} = jVA,$$
$$Q_{\mathrm{se}} = 5.67r_{\mathrm{es}}\left[\left(\frac{T_{\mathrm{s}}}{100}\right)^4 - \left(\frac{T_{\mathrm{e}}}{100}\right)^4\right], \quad C_{\mathrm{e}} = c_{\mathrm{e}}\rho_{\mathrm{e}}s_{\mathrm{e}}A$$

2.2.4. Separator

The temperature of electrode–electrolyte plate is affected by the heat transfer processes (c), (f), and (i). A heat balance is written:

$$C_{\mathrm{s}}\frac{\mathrm{d}T_{\mathrm{s}}}{\mathrm{d}t} = Q_{\mathrm{fs}} + Q_{\mathrm{os}} + Q_{\mathrm{es}} \tag{4}$$

where

$$Q_{\mathrm{fs}} = k_{\mathrm{sf}}A(T_{\mathrm{f}} - T_{\mathrm{s}}), \qquad Q_{\mathrm{os}} = k_{\mathrm{so}}A(T_{\mathrm{o}} - T_{\mathrm{s}}),$$
$$Q_{\mathrm{es}} = 5.67r_{\mathrm{es}}\left[\left(\frac{T_{\mathrm{e}}}{100}\right)^4 - \left(\frac{T_{\mathrm{s}}}{100}\right)^4\right], \quad C_{\mathrm{s}} = c_{\mathrm{s}}\rho_{\mathrm{s}}s_{\mathrm{s}}A$$

A number of additional quantities are defined:

$$\lambda_1 = \frac{k_{\mathrm{ef}}A}{C_{\mathrm{f}}}, \quad \lambda_2 = \frac{k_{\mathrm{sf}}A}{C_{\mathrm{f}}}, \quad \lambda_3 = \frac{k_{\mathrm{eo}}A}{C_{\mathrm{o}}}, \quad \lambda_4 = \frac{k_{\mathrm{so}}A}{C_{\mathrm{o}}},$$
$$\lambda_5 = \frac{k_{\mathrm{ef}}A}{C_{\mathrm{e}}}, \quad \lambda_6 = \frac{k_{\mathrm{eo}}A}{C_{\mathrm{e}}}, \quad \lambda_7 = \frac{5.67r_{\mathrm{es}}A}{100^4C_{\mathrm{e}}},$$
$$\lambda_8 = \frac{VA}{C_{\mathrm{e}}} + \frac{Aq_{\mathrm{H_2O}}}{2FC_{\mathrm{e}}}, \quad \lambda_9 = j, \quad \lambda_{10} = \frac{k_{\mathrm{sf}}A}{C_{\mathrm{s}}},$$
$$\lambda_{11} = \frac{k_{\mathrm{so}}A}{C_{\mathrm{s}}}, \quad \lambda_{12} = \frac{5.67r_{\mathrm{es}}A}{100^4C_{\mathrm{s}}}, \quad \alpha_1 = \frac{c_{\mathrm{in\_f}}\rho_{\mathrm{in\_f}}s_{\mathrm{f}}}{C_{\mathrm{f}}},$$
$$\alpha_2 = \frac{c_{\mathrm{in\_o}}\rho_{\mathrm{in\_o}}s_{\mathrm{o}}}{C_{\mathrm{o}}}$$

In MCFC stack, the state variables are fuel gas temperature x_1, oxidant gas temperature x_2, electrolyte plate temperature x_3, and separator temperature x_4, u_{f} and u_{o} are control inputs:

- The state variable is

$$X = [x_1, x_2, x_3, x_4]^{\mathrm{T}} = [T_{\mathrm{f}}, T_{\mathrm{o}}, T_{\mathrm{e}}, T_{\mathrm{s}}]^{\mathrm{T}}$$

- The manipulated variable is

$$U = [u_1, u_2]^{\mathrm{T}} = [u_{\mathrm{f}}, u_{\mathrm{o}}]^{\mathrm{T}}$$

- The controlled variable is

$$y = \left[y_1, y_2\right]^{\mathrm{T}} = [x_1, x_4]^{\mathrm{T}}$$

Using the above definitions an abbreviated form of equations describing the temperature of fuel cell follows:

$$\dot{X} = f(x) + G(x)U, \qquad y = h(x) = \begin{bmatrix} T_{\mathrm{f}} \\ T_{\mathrm{s}} \end{bmatrix} = \begin{bmatrix} x_1 \\ x_4 \end{bmatrix} \tag{5}$$

where

$$f(x) = \begin{bmatrix} -(\lambda_1 + \lambda_2)x_1 + \lambda_1 x_3 + \lambda_2 x_4 \\ -(\lambda_3 + \lambda_4)x_2 + \lambda_3 x_3 + \lambda_4 x_4 \\ \lambda_5 x_1 + \lambda_6 x_2 - (\lambda_5 + \lambda_6)x_3^4 + \lambda_7 x_4^4 + \lambda_8 \lambda_9 \\ \lambda_{10} x_1 + \lambda_{11} x_2 + \lambda_{12} x_3^4 - (\lambda_{10} + \lambda_{11})x_4 - \lambda_{12} x_4^4 \end{bmatrix},$$

$$G(x) = \begin{bmatrix} \alpha_1(T_{\mathrm{in\_f}} - x_1) & 0 \\ 0 & \alpha_2(T_{\mathrm{in\_o}} - x_2) \\ 0 & 0 \\ 0 & 0 \end{bmatrix}$$

This temperature model will be nonlinear with disturbances and uncertainty as shown later. The main reasons are as follows: (1) there exists load disturbance (the variation of load current); (2) it is difficult to analyze the thermal transfer in a stack due to its complicated construction, so accurate thermal transfer model may not be established; (3) there are many physical parameters to be determined by experiments, and every parameter may be different greatly under different conditions. In this paper we mainly consider the load disturbance d(x,Δj).

Variable structure control (VSC) offers insensitivity to parameter variations, rejection of external load disturbance and fast dynamic response. The temperature model has a normative affine nonlinear form that makes it possible to design a variable structure controller of the MCFC stack.

3. Design controller for MCFC

Our goal is to design decentralized sliding mode control laws for nonlinear temperature model described by Eq. (5). We introduce the input/output linearization method to the variable structure control system, and then a whole decentralized design variable structure control system with rapid-smooth reaching law and sliding mode is constructed.

3.1. Linearization

The input/output linearization method makes the output and input in linear relation by state transition. For a complete description of input/output linearization method and notation used in the following expression, see Ref. [18].

Consider a kind of MIMO nonlinear system as follows:

$$\dot{X} = f(x) + G(x)U, \qquad y = h(x)$$

where$x \in R^n$; $u \in R^m$; $y \in R^m$; $t \in R$; $G = [\, g_1(x) \quad \cdots \quad g_m(x)\,]$ is a matrix of $n \times m$; $f(x) \in R^n$; $g_k(x) \in R^n$ ($k = 1, 2, \ldots, m$). The item $h(x)$ is a smooth vector field.

Now we introduce the symbol of Lie derivative:

$$L_f^0 h_i = h_i,\ L_f^1 h_i = \frac{\partial h_i}{\partial x} f = \frac{\partial L_f^0 h_i}{\partial x} f, \ldots, L_f^k h_i = \frac{\partial L_f^{k-1} h_i}{\partial x} f,$$
$$i = 1, 2, \ldots, m \tag{6}$$

Then define the structure constant (relative rank) r_i:

$$r_i = \min \left\{ j \left| L_{g_k} L_f^{j-1} h_i = \frac{\partial L_f^{j-1} h_i}{\partial x} g_k(x) \neq 0; \right. \right.$$
$$\left. \left. j = 1, 2, \ldots, n;\ k = 1, 2, \ldots, m \right\}, \quad i = 1, 2, \ldots, m \right. \tag{7}$$

Get the time differential of y_1 from Eq. (5):

$$\dot{y}_1 = \frac{\partial h_1(x)}{\partial x}(f(x) + G(x)u) = L_f^1 h_1 + L_{Gu}^1 h_1 \tag{8}$$

where

$$L_f^1 h_1 = \begin{bmatrix} 1 & 0 & 0 & 0 \end{bmatrix} f(x)$$
$$= f_1(x) = -(\lambda_1 + \lambda_2)x_1 + \lambda_1 x_3 + \lambda_2 x_4 \tag{9}$$

$$L_{Gu}^1 h_1 = \begin{bmatrix} 1 & 0 & 0 & 0 \end{bmatrix} G(x)u = \alpha_1(T_{\mathrm{in\_f}} - x_1)u_1 \tag{10}$$

Since $L_{g_1}^1 h_1 = L_{g_1} L_f^0 h_1 \neq 0 (T_{\mathrm{in\_f}} \neq x_1)$, for $y_1 = h_1$ the structure constant (relative rank) $r_1 = 1$.

Get time differential of y_2:

$$\dot{y}_2 = \frac{\partial h_2(x)}{\partial x}(f(x) + G(x)u) = L_f^1 h_2 + L_{Gu}^1 h_2 = L_f^1 h_2 \tag{11}$$

where

$$L_f^1 h_2 = \begin{bmatrix} 0 & 0 & 0 & 1 \end{bmatrix} f(x) = f_4(x) = \lambda_{10} x_1 + \lambda_{11} x_2$$
$$+ \lambda_{12} x_3^4 - (\lambda_{10} + \lambda_{11})x_4 - \lambda_{12} x_4^4 \tag{12}$$

$$L_{Gu}^1 h_2 = \begin{bmatrix} 0 & 0 & 0 & 1 \end{bmatrix} G(x)u = 0 \tag{13}$$

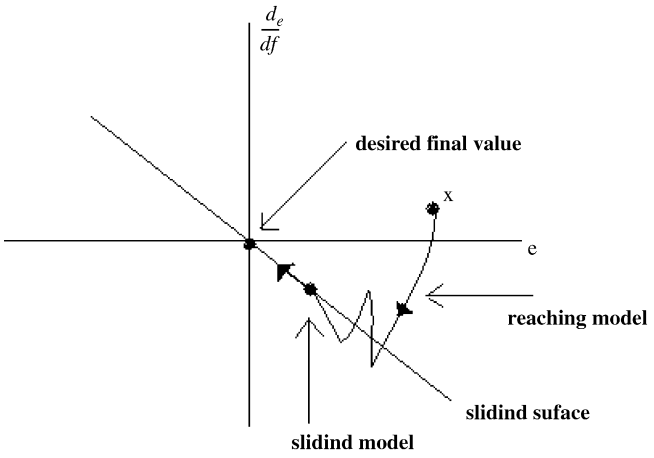

Fig. 2. Graphical interpretation of VSC.

Continue to get time differential of $\dot{y}_2$:

$$\ddot{y}_2 = \frac{\partial L_f^1 h_2}{\partial x}(f(x) + G(x)u) = L_f L_f^1 h_2 + L_{Gu} L_f^1 h_2 \tag{14}$$

where

$$\frac{\partial L_f^1 h_2}{\partial x} = \begin{bmatrix} \lambda_2 \\ \lambda_4 \\ 4\lambda_7 x_4^3 \\ -(\lambda_{10} + \lambda_{11}) - 4\lambda_{12} x_4^3 \end{bmatrix}^T,$$

$$L_f^2 h_2 = L_f L_f^1 h_2 = \begin{bmatrix} \lambda_2 \\ \lambda_4 \\ 4\lambda_7 x_4^3 \\ -(\lambda_{10} + \lambda_{11}) - 4\lambda_{12} x_4^3 \end{bmatrix}^T f(x) \tag{15}$$

$$L_{Gu} L_f^1 h_2 = L_{g_1} L_f^1 h_2 + L_{g_2} L_f^1 h_2 = \lambda_2 \alpha_1 (T_{\text{in\_f}} - x_1) u_1 + \lambda_4 \alpha_2 (T_{\text{in\_o}} - x_2) u_2 \tag{16}$$

Since $L_{Gu} L_f^1 h_2 \neq 0 (T_{\text{in\_f}} \neq x_1$ and $T_{\text{in\_o}} \neq x_2)$, for $y_2 = h_2$ the structure constant (relative rank) $r_2 = 2$. We define a Jacobian matrix J from formulas (10), (13), and (16):

$$J = \begin{bmatrix} L_{g_1} L_f^0 h_1 & L_{g_2} L_f^0 h_1 \\ L_{g_1} L_f^1 h_2 & L_{g_2} L_f^1 h_2 \end{bmatrix} \tag{17}$$

For the actual system (Eq. (5)), J is nonsingular and the characteristic of the zero-dynamics is globally exponential stable. The system can be linearized and stable.

3.2. Obtain the control law of VSC

The design problem consists of selecting the parameters of each structure and defining the traveling logic. The first step is to define a mode $s(t) = 0$, along which the process can slide to its desired final value. The structure of the controller is intentionally altered as its state crosses the mode in accordance with a prescribed control law. Fig. 2 shows graphical interpretation of VSC.

There are many options to choose the sliding mode; the $s(t)$ selected in this work, is a rapid-convergent sliding mode presented in Ref. [17].

The sliding mode is

$$s = \varphi(p)e + \varsigma e^{\beta} \tag{18}$$

where: $\varphi(p) = p + \psi$ and $p = \text{d}/\text{dt}$ is differential operator; $\psi > 0$; $0 < \beta = \beta_1/\beta_2 < 1$, β_1 and β_2 $(\beta_1 < \beta_2)$ are positive odd numbers and tuning parameter, which helps to define s, and e is the tracking error.

The objective of control is to ensure that the controlled variable be equal to its reference value at all times, meaning that e and its derivatives must be zero. The reaching law [17] is chosen as

$$\dot{s} = -\varepsilon |s|^{\alpha} \text{sgn}(s) - ks, \varepsilon, k > 0, 1 > \alpha > 0 \tag{19}$$

where the $-\varepsilon |s|^{\alpha} \text{sgn}(s)$ item is the sufficient condition for s to have sliding mode, so $s \to 0$ in limited time. $|s|^{\alpha}$ acts as the "smooth" function and $-ks$ guarantees rapid reaching velocity.

Formulas (18) and (19) have the same structure, with the corresponding relation: $k \leftrightarrow \psi$, $\alpha \leftrightarrow \beta$, $\varepsilon \leftrightarrow \varsigma$.

Once the sliding mode has been selected, attention must be turned to the design of the control law that drives the controlled variable to its reference value and satisfies.

For the MIMO system (5), we define the number of switch function equal to the number of control input, $m = 2$. The switch function can be represented as

$$s(x) = \begin{bmatrix} s_1(x) & s_2(x) \end{bmatrix}^{\text{T}} \tag{20}$$

The switch surface is

$$S_i = \{x | s_i(x) = 0\}, \quad i = 1, 2$$

Using decentralized variable structure control scheme, we design the switching function s_i according to the structure constant r_i of y_i.

Considering the structure constant $r_1 = 1$, $r_2 = 2$ calculated in Section 3.1, we get

$$s_1 = \varphi_1(p)e_1 + \varsigma_i e_i^{\beta} \quad (0 < \beta < 1) \tag{21}$$

where

$$\varphi_1(p) = p^1 + \psi_{1,1}, \qquad e_1 = \int_0^t (y_1 - y_{\text{d1}}) \text{d}t,$$

$$s_2 = \varphi_2(p)e_2 + \varsigma_2 e_2^{\beta} \tag{22}$$

where

$$\varphi_2(p) = p^2 + \psi_{2,1} p^1 + \psi_{2,2}, \qquad e_2 = \int_0^t (y_2 - y_{\text{d2}}) \text{d}t$$

The $y_{\text{d}} = [y_{\text{d1}}, y_{\text{d2}}]$ is the desired output; $\psi_{i,0} = 1$; $\psi_{i,1}$, $\psi_{i,2}, \ldots, y_{i,r_i}$ are constants, whose numerical values determine the probability of output error on the sliding mode.From (5), (17), (21) and (22), we can get the time differential of vector s_i is

$$\dot{s} = A(x) + Ju - \varphi(p)y_d + \begin{bmatrix} \varsigma_1\beta\left[\int_0^t (y_1 - y_{d1})dt\right]^{\beta-1}(y_1 - y_{d1}) \\ \varsigma_2\beta\left[\int_0^t (y_2 - y_{d2})dt\right]^{\beta-1}(y_2 - y_{d2}) \end{bmatrix} \quad (23)$$

where

$$A(x) = \begin{bmatrix} \sum_{j=0}^{r_1}\psi_{1,j}L_f^{r_1-j}h_1(x) \\ \sum_{j=0}^{r_2}\psi_{2,j}L_f^{r_2-j}h_2(x) \end{bmatrix} \psi_{1,0} = 1, \psi_{2,0} = 1 \times \begin{bmatrix} L_f^1 h_1(x) + \psi_{1,1}h_1(x) \\ L_f^2 h_2(x) + \psi_{2,1}L_f^1 h_2(x) + \psi_{2,2}h_2(x) \end{bmatrix},$$

$$\varphi(p)y_d = \begin{bmatrix} \varphi_1(p)y_{d1} \\ \varphi_2(p)y_{d2} \end{bmatrix}$$

Taking (19) into (23), we can get the control law as

$$\begin{aligned} \begin{bmatrix} u_1 \\ u_2 \end{bmatrix} &= J^{-1}\left\{ \begin{bmatrix} -\varepsilon|s_1|^\alpha \mathrm{sgn}(s_1) - ks_1 \\ -\varepsilon|s_2|^\alpha \mathrm{sgn}(s_2) - ks_2 \end{bmatrix} - A(x) + \varphi(p)y_d \right. \\ &\quad \left. - \begin{bmatrix} \varsigma_1\beta\left[\int_0^t (x_1 - y_{d1})dt\right]^{\beta-1}(x_1 - y_{d1}) \\ \varsigma_2\beta\left[\int_0^t (x_4 - y_{d2})dt\right]^{\beta-1}(x_4 - y_{d2}) \end{bmatrix} \right\} \\ &= J^{-1} \times \left\{ \begin{bmatrix} -\varepsilon|s_1|^\alpha \mathrm{sgn}(s_1) - ks_1 \\ -\varepsilon|s_1|^\alpha \mathrm{sgn}(s_2) - ks_2 \end{bmatrix} \right. \\ &\quad - \begin{bmatrix} L_f^1 h_1(x) + \psi_{1,1}h_1(x) \\ L_f^2 h_2(x) + \psi_{2,1}L_f^1 h_2(x) + \psi_{2,2}h_2(x) \end{bmatrix} \\ &\quad + \begin{bmatrix} \varphi_1(p)y_{d1} \\ \varphi_2(p)y_{d2} \end{bmatrix} \\ &\quad \left. - \begin{bmatrix} \varsigma_1\beta\left[\int_0^t (x_1 - y_{d1})dt\right]^{\beta-1}(x_1 - y_{d1}) \\ \varsigma_2\beta\left[\int_0^t (x_4 - y_{d2})dt\right]^{\beta-1}(x_4 - y_{d2}) \end{bmatrix} \right\} \end{aligned} \quad (24)$$

where $L_f^1 h_1(x)$, $L_f^1 h_2(x)$ and $L_f^2 h_2(x)$ are calculated respectively by (8), (12), and (15); s_1 and s_2 are obtained respectively from (21) and (22).

Here is the input design of the variable structure control of nonlinear temperature system (5). The robustness of the normative affine nonlinear system with chattering is proved in [17]. Selecting parameters of the sliding mode and those of the reaching law are considered as one of the main underlying problems associated with VSC. This is accomplished by formulating the VSC parameters selection as an optimization problem and genetic algorithm (GA) are used in the optimization process.

3.3. Optimize the parameters of controller

Genetic algorithm (GA) is directed random search techniques which can find the global optimal solution in complex multidimensional search spaces. GA was first proposed by Holland [19] and has been applied successfully to many engineering and optimization problems [20,21]. It is a searching algorithm based on natural selection and species heredity. While simulating the hereditary behavior of natural biology, such as aberrance and competition, GA improves the solution of a problem, and obtains a satisfying or optimum solution. There are basically three genetic operators used to generate and explore the neighborhood of a population and select a new generation. These operators are selection, crossover and mutation. More details about GA can be found in [22].

In this paper, GA is used to optimize the parameters of variable structure control, including the parameters of the sliding mode and those of the reaching law. The parameters searched for optimum values are $\varphi_{2,1}$, $\varphi_{1,2}$, ς_1, β, $\varphi_{1,1}$, ς_2, ε, k and α. To start the proposed GA method, a performance index must be defined. The selection of the performance index depends on the objective of the control problem. The procedure described the use of GA in optimizing the parameters of variable structure control is summarized as follows:

(1) Determining the ranges of parameters of VSC based on experience, and generating the initial population.
(2) Evaluate some performance index for all optimized parameters generated in step 1. In the present work, the following index is selected:

$$\min \int_0^T \left\{(x - x_d)^T W_1 (x - x_d) + u^T W_2 u\right\} dt$$

where W_1 and W_2 are the weighting coefficients, and x_d is the vector of steady state operation.
(3) Use genetic operators (selection, crossover, mutation) to produce new generation of parameters of VSC.
(4) Evaluate the performance index in step 2 for the new generation of parameters of VSC. Stop if there is no more improvement in the value of the performance index or if certain predetermined number of generation has been used, otherwise go to step (3).

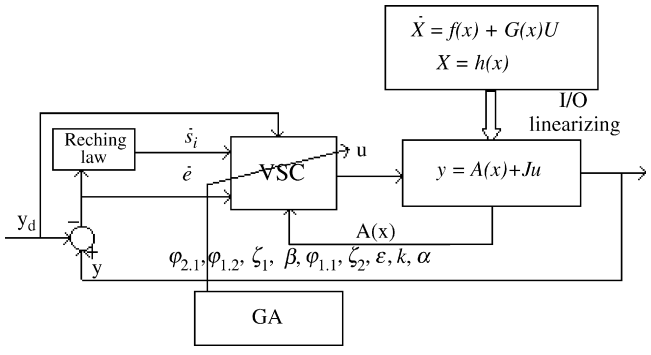

Fig. 3. Illustration of temperature control.

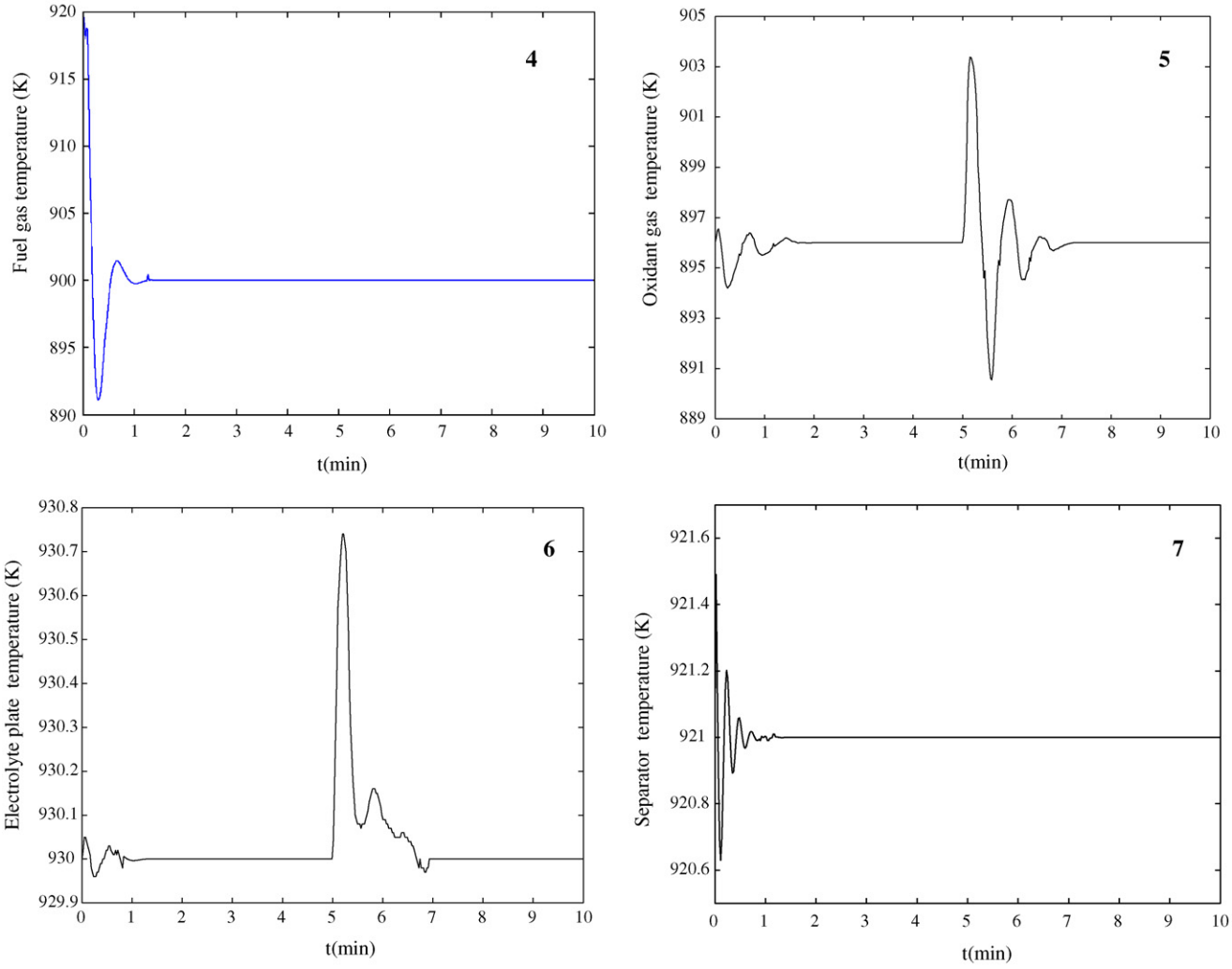

Figs. 4–7. Trajectories of MCFC temperature variable.

4. Simulation

In this section, we present numerical experiments to show the validation of the proposed variable structure control based on the dynamic thermal model of MCFC. The detailed parameters about MCFC stack used for simulation can be found in [8]. The structure of VSC for MCFC temperature control system is shown in Fig. 3.

In normal working condition, the current density $j_0 = 1500\,\mathrm{A\,m^{-2}}$. The steady output value of the operating temperature of the MCFC stack is $x_\mathrm{d} = \begin{bmatrix} 900 & 896 & 930 & 921 \end{bmatrix}^T$ K. We assume that there exist an initial fuel gas temperature error 20 K ($x_1^0 = 920\,\mathrm{K}$) and a step disturbance Δj with the value of $150\,\mathrm{A\,m^{-2}}$ (equal to 10% of regular condition) at the fifth minutes. The variable structure controller is used to adjust the stack temperature to its steady value.

To start the proposed algorithm, a decision has to be made about the GA parameters which include population size, crossover probability, mutation probability, and number of generations. General guidelines available in the literature can be used in the selection process of the GA parameters [22,23]. After so many trials, a population size of 90, a crossover probability of 0.7, and a mutation probability of 0.001 are used. Using the GA design procedure described in Section 3.3, initial range and optimal value of control law parameter that minimize the performance indices are, given by

$$\varphi_{1,1} = 5.6(1\text{–}20), \quad \varsigma_1 = 1(0.1\text{–}3), \quad \varphi_{2,1} = 10(1\text{–}15),$$
$$\varphi_{2,2} = 26(0.1\text{–}30), \quad \beta = 0.7(0.1\text{–}0.9), \quad \varsigma_2 = 1(0.1, 3),$$
$$\varepsilon = 1(0.1\text{–}2), \quad k = 6(1\text{–}20), \quad \alpha = 0.8(0.1\text{–}0.9)$$

With the control of VSC, we get a group of the MCFC temperature trajectories. The trajectories of fuel gas temperature (x_1), oxidant gas temperature (x_2), electrolyte plate temperature (x_3) and separator temperature (x_4) are showed respectively in Figs. 4–7. Above results show that the temperature can track a given temperature reference value well. The temperature fluctuations of stack only occur when current density changes suddenly, the fluctuations attenuate gradually, and the temperatures achieve the controlling accuracy after a short period of time. The upper temperatures are within safety area. The tem-

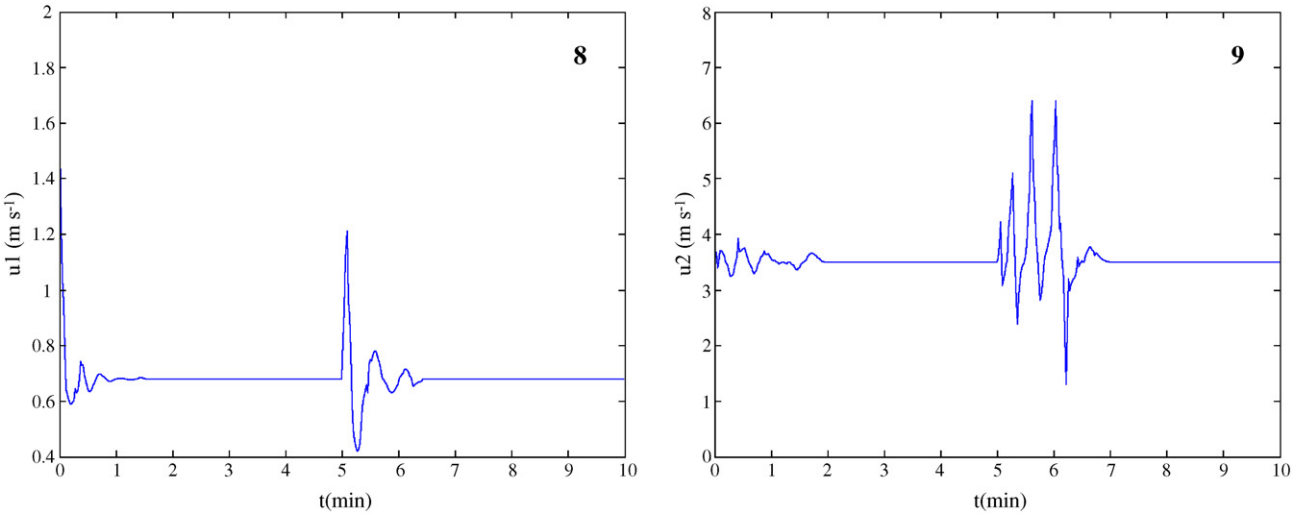

Figs. 8 and 9. Curves of manipulated variable u_1 and u_2.

perature error of the fuel gas is less than 11 K, the electrolyte plate is less than 1 K and the error of oxidant gas is less than 12 K, and these conditions are permitted in MCFC stacks. The fuel gas temperature and separator temperature x_4 (output y_2) are robust to the current disturbance and the sliding modes s_1 and s_2 are invariant to disturbance. From Figs. 8 and 9, velocities of fuel gas (u_1) and oxidant gas (u_2) are within the area of control (the fuel gas velocity: 0–2 m s^{-1}, and oxidant gas velocity: 0–8 m s^{-1}). Above simulation results show that the control system can reach stable finally, and its dynamic characteristics are fairly good, and it is robust to the disturbance.

5. Conclusion

The operating temperature of the stack is the most important variable which is controlled in the MCFC system. However, the existing mechanism model is too complicated to meet the design requirements of the control system, and less model-based control strategy is discussed in past works. According to the demand of controlling the temperature of MCFC stack, normative affine nonlinear model of MCFC temperature characteristic considering the disturbance and uncertainty is analyzed based on the modeling of Shen [8]. A model-based variable structure control (VSC) with GA is presented for MCFC. Variable structure control is a special discontinuous control technique applicable to a broad variety of practical systems due to its easy implementation and good robustness to unmodeled dynamics, parameter variations and external disturbances. We introduce the input/output linearization method to the variable structure control system, and design decentralized variable structure control system with optimized parameters by GA. Simulation results show that the method presented in the paper can control the operating temperature to reach the target value quickly, which verified the effectiveness and robustness of it.

References

[1] M. Bischoff, Molten carbonate fuel cells: A high temperature fuel cell on the edge to commercialization, J. Power Sources 160 (2) (2006) 842–845.
[2] J.H. Koh, B.S. Kang, H.C. Lim, J. Power Sources 91 (2) (2000) 161–171.
[3] B. Bosio, P. Costamagna, F. Parodi, J. Chem. Eng. Sci. 54 (13–14) (1999) 2907–2916.
[4] J.-H. Koh, H.-K. Seo, Y.-S. Yoo, H.C. Lim, J. Chem. Eng. Sci. 87 (3) (2002) 367–379.
[5] F. Standaert, K. Hemmes, N. Woudstra, J. Power Sources 70 (2) (1998) 181–199.
[6] W. He, Q. Chen, J. Power Sources 73 (2) (1998) 182–192.
[7] M.D. Lukas, K.Y. Lee, H. Ghezel-Ayagh, IEEE Trans. Energy Convers. 14 (4) (1999) 1651–1657.
[8] C. Shen, G.-Y. Cao, X.-J. Zhu, Int. J. Energy Res. 28 (2004) 403–410.
[9] F. Yoshiba, N. Ono, Y. Izaki, Y. Watanabe, T. Abe, J. Power Sources 71 (1) (1998) 328–336.
[10] J.M. Smith, H.C. van Ness, Introduction to Chemical Engineering Thermodynamic, McGraw-Hill, New York, 1987.
[11] A. Jaime, O. Pernilla, S. Azra, J. Power Sources 112 (1) (2002) 54–60.
[12] R.A. DeCarlo, S.H. Zak, G.P. Matthews, Proc. IEEE 76 (3) (1988) 212–232.
[13] J.Y. Hung, W.B. Gao, J.C. Hung, IEEE Trans. Ind. Electron. 40 (1) (1993) 2–22.
[14] K.-K. Shyu, C.-Y. Liu, J. Guidance Control Dyn. 19 (6) (1996) 1395–1397.
[15] K.-K. Shyu, K.-C. Hsu, W.-J. Liu, Proceedings of the 2004 IEEE Taipei, Taiwan, March 21–23, International Conference OD Networking, Sensing Control, 2004.
[16] F. Zheng, Q.-G. Wang, T.H. Lee, IEEE TranS. Fuzzy Syst. 10 (6) (2002) 686–697.
[17] X. Chun-shan, S. Xing-jin, C. Guang-yi, J. Comput. Simulat. 21 (7) (2004) 115–119.
[18] Y.-M. Hu, Nonlinear Control Systems Theory and Applications, National Defence Industry Press, Beijing, 2002, pp. 115–118.
[19] J.H. Holland, Adapation in Natural and Artificial Systems, University of Michigan Press, Ann Arbor, MI, 1975.
[20] B. Porter, A. Jones, Electron. Lett. 28 (9) (1992) 843–844.
[21] J. Lansberry, L. Wozniak, D. Goldberg, IEEE Trans. Automat. Control 7 (1992) 623–630.
[22] L. Davis, The Handbook of Genetic Algorithms, Van Nostrand Reinhold, New York, 1991.
[23] D. Goldberg, Genetic Algorithms in Search Optimization and Machine Learning, Addison-Wesley, Reading, MA, 1989.